Research on vibration property of Picea wood for piano sound quality neural network and ant colony algorithm

Yang Yang
Harbin University
Shi Jie
Northeast Forestry University
Guo Yanling (GuoYanlingLaoshi@163.com)
Northeast Forestry University
Liu Zhenbo
Northeast Forestry University

Research Article

Keywords: Wood Vibration Performance, Piano Soundboard, Acoustic Quality, Forecast, Neural Network

Posted Date: September 27th, 2023

DOI: https://doi.org/10.21203/rs.3.rs-3372594/v1

Additional Declarations: No competing interests reported.

Research on vibration property of Picea wood for piano sound quality neural network and ant colony algorithm

Yang Yang [1,2],Shi Jie[3], Guo Yanling[2], Liu Zhenbo[4]
Corresponding editor: Guo Yanling, Liu Zhenbo
GuoYanlingLaoshi@163.com;
1 College of art and design, Harbin University, Harbin 150076, China
2 College of Mechanical and Electrical Engineering, Northeast Forestry University, Harbin 150040, China
3 College of Computer and Control Engineering, Northeast Forestry University, Harbin 150040, China
4 College of Materials Science and Engineering, Northeast Forestry University, Harbin 150040, China
Abstract With its characteristics of wide range and large volume variation, piano has an unshakable position in the Musical Instruments and is widely loved by numerous people. In a upright piano, the basic function of the piano sound board (resonance board) is used to expand the sound emitted by the string. Different wood species would produce different vibration amplitudes and resonance effects. If the other parts of the two pianos are exactly the same, their advantages and weaknesses can only be determined by the resonance board, so the resonance version of the material is particularly important. Based on the vibration theory of piano resonance plate, this study analyzed the vibration characteristics of the resonance plate and used the BP neural network ACO-BP optimized by ant colony algorithm. Using the dynamic elastic modulus, the elastic modulus and shear modulus ratio, acoustic radiation damping coefficient and acoustic impedance of the wood species of Russian Far East Picea koraiensis Nakai, Picea jezoensis, Picea spinlosa and Picea sitchensis Carr. as the prediction inputs, the accuracy of the model for predicting the musical instrument grade reached 95%. It is of great value for improving the acoustic quality of piano by establishing the corresponding acoustic quality evaluation system of national Musical Instruments and deeply investigating the prediction method of the parameters of the acoustic evaluation system to realize the transition from the subjective evaluation to objective evaluation.
Keywords Wood Vibration Performance; Piano Soundboard; Acoustic Quality; Forecast; Neural Network

Introduction

In the past few years, a number of musicians, scientists and instrument makers have studied the microscopic properties of different wood species, laying the foundation for the selection of musical instrument sound boards.

At present, the quality of soundboards depends on subjective evaluation, which is not always accurate and effective[1,2]. The knowledge in this field comes from both scientific methods and empirical methods, and sometimes, as defined by Woodhouse[3] through "lasting folk memory". The purpose of any research is carried out to determine the mechanical and micro-structural properties of wood in order to relate them to the resonant macroscopic behavior to obtain measurable quantities[4-6]. For example, as well know, the modulus of the front and back panels of the Poplar violin must be accurately evaluated[7]. Related to this, Bremaud reported in his completed work[8,9] that, "From the perspective of engineering science, people can make a quite firm statement that the "resonant wood" of spruce naturally had very high axial and anisotropic properties, and low (but not extreme) density and tangent of power loss angle.

In order to provide a more reliable scientific basis for the material selection of the actual piano resonance plate production, it is necessary to study the vibration characteristics of the wood used for the actual size of the piano resonance plate. It is of great significance to establish the corresponding acoustic quality evaluation system for national Musical Instruments, to develop the prediction method of the parameters of the acoustic evaluation system, to realize the transition from the subjective evaluation to objective evaluation of musical instrument selection, and to improve the acoustic quality of piano. Norimoto M., Sugiyama M., Kubojima Y.[10-16] et al(1983-2000). evaluated the vibration performance of wood used for musical instrument sound boards. Specific dynamic elastic modulus, tangent of dynamic loss Angle, acoustic radiation damping coefficient R, acoustic impedance and energy loss parameters per vibration period have the most significant effects on the acoustic vibration performance of wood. Liu Yixing, Liu Zhenbo et al(2005). used the AHP, comprehensive coordinate method and comprehensive scoring method to evaluate the vibration performance of resonant source material of piano and other Musical Instruments. Christoph[17] (1998)used the subjective scoring method to grade violins in terms of acoustic adaptability, aesthetic suitability and overall wood vibration quality. Then the material properties were measured from the aspects of sound velocity, sound attenuation, resonance frequency, specific dynamic elastic modulus, hardness, density, tracheid diameter and wall thickness, microfiber angle, ring width, ring width variation coefficient, late wood rate, fiber length, dimensional stability, etc., and the properties of the measured materials were analyzed by the multiple linear regression method.

Currently, with the rise of neural networks, more and more fields have carried out research on artificial intelligence in their fields. The above methods are all mathematical methods, which lack accuracy and systematic prediction models for predicting the performance of piano soundboard materials. In this study, the BP neural network[18] optimized based on ant colony algorithm[19] was proposed to make up for the shortcomings such as easy to fall into local areas, so that the algorithm can be applied with high precision prediction, strong adaptability and application range, and can effectively reduce errors and improve the accuracy of prediction.

Theory

Wood board is an anisotropic material. As a resonant plate of an upright piano, its length and width are much larger than its thickness. Therefore, the anisotropic rectangular thin plate vibration theory can be applied to solve the vibration characteristics of the musical instrument resonator plate. According to generalized Hooke's law, the physical equation of anisotropic elastomers is simplified to obtain Eq. (1):

$$\begin{aligned} \sigma_x &= \frac{1}{1-\mu_x\mu_y}(E_x\varepsilon_x + \mu_x E_y \varepsilon_y) \\ \sigma_y &= \frac{1}{1-\mu_x\mu_y}(E_y\varepsilon_y + \mu_y E_x \varepsilon_x) \\ \tau_{xy} &= G\gamma_{xy} \end{aligned} \quad (1)$$

Where, σ_x, σ_y are the stresses in the directions x and y; μ_x, μ_y are the Poisson's ratios of the directions x and y; $\varepsilon_x, \varepsilon_y$ represent the strains in the x and y directions; G is the shear modulus, $G = \rho V^2$, V is the surface wave propagation velocity (m/s) of the resonant source material; τ_{xy} is the shear stress; γ_{xy} is the shear strain.

The geometric equation of thin plate with small deflection is described as Eq. (2):

$$\begin{aligned} \varepsilon_x &= -z\frac{\partial^2 w}{\partial x^2} \\ \varepsilon_y &= -z\frac{\partial^2 w}{\partial y^2} \\ \gamma_{xy} &= -2z\frac{\partial^2 w}{\partial x \partial y} \end{aligned} \quad (2)$$

Eq. (2) was substituted into Eq. (2) to obtain Eq. (3):

$$\begin{aligned} M_x &= \int_{-k/2}^{k/2} \sigma_x z dz = -D_{11}\left(\frac{\partial^2 w}{\partial x^2} + \mu_y \frac{\partial^2 w}{\partial y^2}\right) \\ M_y &= \int_{-k/2}^{k/2} \sigma_y z dz = -D_{22}\left(\frac{\partial^2 w}{\partial y^2} + \mu_y \frac{\partial^2 w}{\partial x^2}\right) \\ M_{xy} &= \int_{-k/2}^{k/2} \tau_{xy} z dz = -2D_{66}\frac{\partial^2 w}{\partial x \partial y} \end{aligned} \quad (3)$$

Where D_{11} and D_{22} are the flexural rigidity of the thin plate in the elastic direction and D_{66} is the torsional stiffness in the natural direction, and the all three are called principal stiffness, as shown in Eq. (4):

$$D_{11} = \frac{E_x h^3}{12(1-\mu_x\mu_y)}$$
$$D_{22} = \frac{E_y h^3}{12(1-\mu_x\mu_y)} \quad (4)$$
$$D_{66} = \frac{G_{xy} h^3}{12}$$

Therefore, the differential equation of transverse free vibration of orthotropic thin plates can be obtained as follows:

$$D_{11}\frac{\partial^4 w}{\partial x^4} + 2(D_{12} + 2D_{66})\frac{\partial^4 w}{\partial x^2 \partial y^2} + D_{22}\frac{\partial^4 w}{\partial y^4} - \frac{\rho\omega^2}{g}w = 0 \quad (5)$$

Materials and methods

Picea wood is one of the main tree species for making piano soundboards. Pianos are basically made of wood with a length of 2000mm and a width of more than 120. The actual material properties for producing piano resonance boards are shown in Table 1:

Table 1 Parameters of length, width and thickness and air-dried density of various wood species

tree species	Place of Origin	length	width/mm	thickness/ mm	air-dry density/g·cm^{-3}
Russian Far East Picea koraiensis Nakai	Komsomolsk-on-Amur of Russian	2000~2400	120~135	11.0~12.6	0.375~0.542
Picea jezoensis	the Changbai mountains				0.372~0.467
Picea spinlosa	Bomi of Tibet				0.325~0.562
Picea sitchensis Carr.	the Charlotte Island of North America				0.385~0.449

The vibration characteristics of piano resonant source material were examined based on the vibration theory of beam. The acoustic vibration characteristic parameters (specific dynamic modulus of elasticity, ratio of elastic modulus to shear modulus, acoustic radiation resistance coefficient, acoustic impedance, surface wave propagation velocity, etc.) of resonant source material were measured by tapping acoustic vibration experiment method, longitudinal resonance, and surface wave propagation method.

I. Examination of vibration mode and surface wave propagation velocity of piano resonant plate

After manual selection of 20 groups of white fish scale spruce sound board raw materials by material selection technicians, five groups of resonance board materials with different vibration properties were selected, which inclined the one that glued together into piano resonance board. The piano to be produced in this research was an upright piano of model 121, whose resonant plate size was 1408mm (x-direction) ×937mm (y-direction) × 8mm (thickness). The values in the length and width directions were much larger than that in the thickness direction, which can be regarded as a thin plate, because the vibration mode of the plate was much more complex than that of the beam. Therefore, if

the vibration theory of beam was used to determine the vibration mode, it was not accurate enough and necessary to use the vibration mode based on the plate.
In order to accurately measure the vibration frequencies of piano resonator plates, two supporting methods were adopted, as shown in Figs.1 and 2. The vibration of the plate was complicated and difficult to obtain the vibration frequency of each order and the surface wave propagation speed by a simple measurement, because the two support modes were measured by multiple points. In this experiment, a total of 4×4 points were measured, as shown in Table 2.

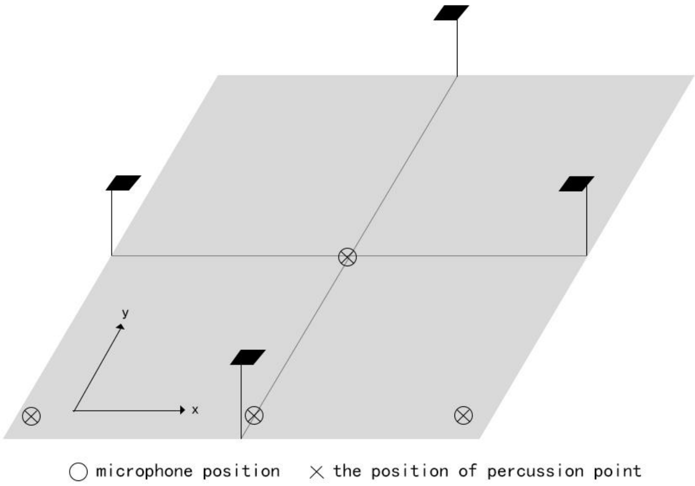

Fig. 1 Vibration frequency of piano resonant plate and surface wave propagation velocity of resonant source material

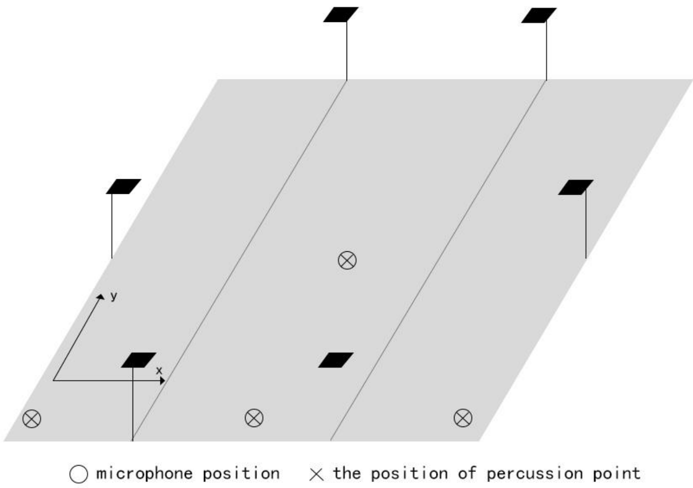

Fig. 2 Vibration frequency of piano resonant plate and surface wave propagation velocity of resonant source material
Table 2 Vibration measurement position of piano resonator plate

Percussion point / Microphone	1	2	3	4
1	11	12	13	14
2	21	22	23	24
3	31	32	33	34
4	41	42	43	44

II. Density measurement

In this study, a high-precision automatic wood density measuring instrument, AU-300CE, was used that was manufactured by the Hangzhou Goldmic Instrument Co., Ltd., China

III. Measurement of dynamic elastic modulus and specific dynamic elastic modulus of resonant source materials

The test principle of vibration frequency measurement of test specimens is shown in Fig. 3. The resonant source material was supported with a foam at the vibration frequency node corresponding to it, and the microphone with high sensitivity, wide band, and low noise was placed on one end of the specimen. Then the blade with a rotating shaft at the end was turned to hit the other end or the middle of the specimen. The collected signals were amplified and filtered by the microphone and then transmitted to the FFT analyzer to obtain the resonance frequencies. The measured resonance frequency can be used to calculate the dynamic elastic modulus (Eq. 6), and then the main parameters characterizing the vibration characteristics of the resonant source material - specific dynamic elastic modulus, acoustic radiation damping, acoustic impedance, etc.

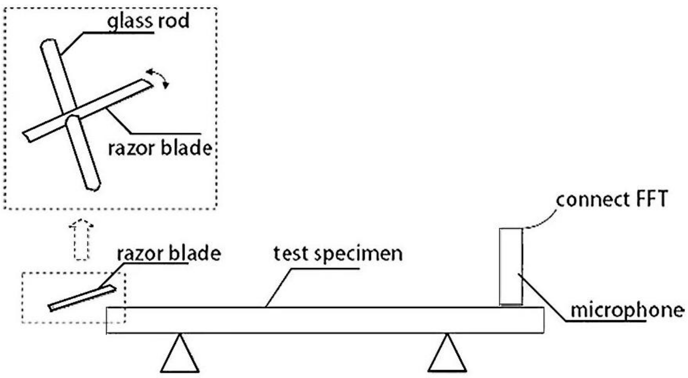

Fig 3. Experimental principle of resonant frequency measurement of resonant source material

The dynamic elastic modulus of the resonant source material was calculated as follows:

$$E = \frac{48\pi^2 L^4 \rho f^2}{\beta^4 h^2} \tag{6}$$

Where: E - Dynamic elastic modulus (GPa) of resonant source material; f - Resonance frequency of the resonant source material (Hz); L- Length of resonant source material (m): β - thickness of resonant source material (m); ρ - density of resonant source material (kg· m); m- The coefficient determined by the order of vibration.

According to the dynamic elastic modulus of E is the resonance plate material calculated in Eq. 6. According to Eq. 6, the ratio of wood density to the specific dynamic elastic modulus of wood was obtained.

IV. Examination of shear modulus of piano resonant source material

In this experiment, the shear modulus was measured by the surface wave propagation method. The experimental principle of surface wave propagation is shown in Fig. 4. The wood specimen was supported with a foam at the fundamental frequency vibration node corresponding to it, and the sensor was fixed at both ends of the specimen, and then the blade with a rotating shaft at the end was turned to knock one end of the specimen, and the other end of the specimen captured the surface wave, and the trigger signal and the received signal were transmitted by the high-precision sensor to the FFT analyzer for analysis, and the time difference was obtained. The shear modulus of the specimen was calculated by Eq. 7.

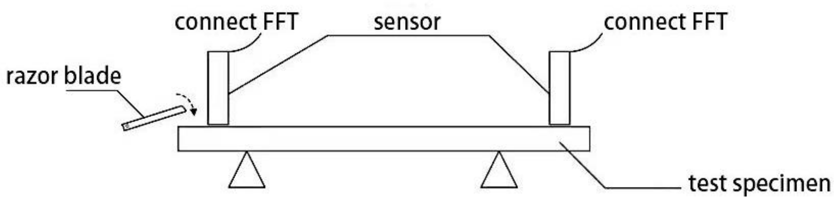

Fig. 4 Schematic diagram of shear modulus measurement experiment

$$G = \rho V^2 \tag{7}$$

Where: G is the dynamic shear modulus (GPa) of the resonant source material; ρ is the density of the resonant source material; V is the surface wave propagation speed of the resonant source material.

According to Eq.6, the ratio of dynamic elastic modulus to dynamic rigid modulus E/G can be calculated from the dynamic elastic modulus E and shear modulus G to characterize the sound color of the musical instrument soundboard.

V. Calculation of sound amplitude damping coefficient R

The Sound amplitude damping coefficient R (referred to as sound amplitude damping, also known as sound radiation quality constant) showed the acoustic radiation capacity of wood and wood products, that is, the size of the acoustic power radiated to the surrounding air, which is proportional to the speed of sound transmission and inversely proportional to the density of wood.

$$R = \frac{v}{\rho} = \sqrt{\frac{E}{\rho^3}} \tag{8}$$

R is often an important parameter for people to evaluate the sound amplitude quality of wood. When wood is used as a sounding board for musical instruments, wood with higher R should be selected. When the density of wood is too high, R tends to be smaller.

VI. Calculation of acoustic impedance

Acoustic impedance of wood is the product of the density of wood and the sound velocity of wood.

$$\omega = \rho v = \sqrt{\rho E} \tag{9}$$

The acoustic impedance of wood is an important physical quantity that characterizes the properties of the medium and plays an important role in the propagation of sound, especially the propagation at the junction of two media. In this study, for piano sound boards, the lower the wood density, the higher the R.

Some of the information is shown in Table 3.

Table 3 Vibration source material indexes of each tree species (part)

	ρ	E/G	E/ρ	R	ω
Russian Far East Picea koraiensis Nakai A1	1.108	0.888	0.732	0.857	1.043
Picea jezoensis B1	0.984	0.843	0.605	0.933	0.903
Picea spinlosa C1	1.020	0.861	0.813	0.905	0.946
Picea sitchensis Carr. D1	1.051	0.873	0.766	0.891	0.980

ACO-BP

BP neural network

BP neural network is one of the most widely used multi-layer feedforward neural networks in artificial neural networks, and its network structure is shown in Fig. 5.

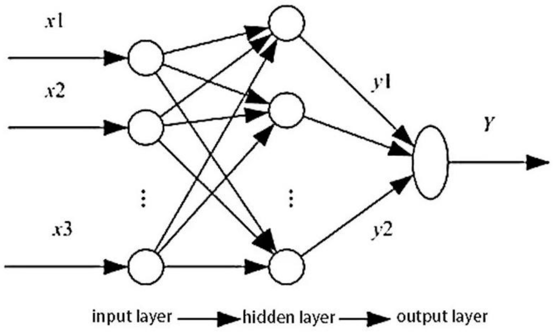

Fig. 5 BP neural network structure diagram

The neural network is composed of an input layer, several hidden layers and output layers, and the connection mode of nodes between adjacent layers is full connection. For each node of the hidden layer and output layer, the relation between input and output is as follows:

$$y_i = f_i\left(\sum_{j=1}^{n} \omega_{ij} x_j - \theta_i\right) \tag{10}$$

Where, f_i is the activation function of node i, usually the Sigmoid function or SoftMax function, y_i is the output value of node i, ω_{ij} is the connection weight of node j to node i, x_j is the output value of node j, and θ_i is the bias value of node i.

The training of BP neural network belongs to supervised training. Its basic idea is to input sample features into the input layer of the network and pass them into the output layer after processing by the hidden layer. Then, the errors of output and sample labels are backpropagated.

At the kth iteration, the node parameter update Equation is as follows:

$$\omega_{ij}(k+1) = \omega_{ij}(k) - \eta \nabla E(k) = \omega_{ij}(k) - \eta \frac{\partial E^k(\omega)}{\partial \omega_{ij}} \tag{11}$$

η is the learning rate.

ACO optimization

In each iteration of the ACO-BP algorithm, several ants in the ant colony selected the weight and bias of each node according to the pheromone table, inputted the sample characteristic value after the selection, the network output was obtained, the pheromone table was updated according to the loss function value, and carry out local optimization with the help of BP algorithm.

In a neural network, the total number of node parameters $l = n_h(n_i + 1) + n_o(n_h + 1)$, n_h, n_i, and n_o was the number of nodes in the input layer, hidden layer, and output layer, respectively. Within the range of parameters A and B of each node, the discrete points D(h=1, 2, ..., d) with a number of C were selected, and the values of these discrete points obey normal distribution. Each point A had its corresponding pheromone value B, being stored in the pheromone matrix, where the initial value of each item is:

$$\tau_{ijh} \leftarrow 1/(n_i + n_h + n_o) \tag{12}$$

For each node parameter, each ant selected a discrete point and stored the selection in the local storage of the ant. The storage dimension of an ant was determined by the node parameters in the network.

When each ant selected ω_{ij} value, it decided whether to select a new value according to the probability of $1-q$, where q was a parameter in the decision rule, and the probability of selecting a discrete point a_{ijh} is:

$$p_{ijh} = \frac{\tau_{ijk}}{\sum_{k=1}^{d} \tau_{ijk}} \tag{13}$$

After all ants selected node parameters, pheromone updates began. Only the optimal ants (those with the least loss function) released pheromones along their chosen path, as follows.

$$\begin{aligned} \tau_{ijh} &= \tau_{ijh} + \Delta\tau_{ijh}^{\text{best}}, \forall a_{ijh} \in T_{\text{best}} \\ \Delta\tau_{ijh}^{\text{best}} &= 1/E^{\text{best}} \end{aligned} \tag{14}$$

Where T_{best} is the solution constructed by the best ant so far, and E^{best} is the loss function value of the best ant.

After the optimal ant pheromone was released, the pheromone volatilization step was carried out to reduce all the values in the pheromone table, as shown in Eq. 16.

$$\tau_{ijh} \leftarrow (1-\rho)\tau_{ijh}, \forall a_{ijh} \tag{15}$$

Where is a constant, indicating the volatilization rate of pheromone.

In the pheromone updating step, the pheromone value is limited to the interval, where it is expressed by Eqs. 16 and 17.

$$\tau_{max} = 1/(\rho E^{\text{best}}) \tag{16}$$

$$\tau_{min} = \tau_{max}/(2l) \tag{17}$$

Evaluation index

In order to evaluate the training and prediction errors of ACO-BP neural network, the mean square error (MSE) index was used as the measurement standard when verifying the training and prediction errors.

$$MSE = \frac{1}{n}\sum_{i=1}^{n}(X_i - Y_i)^2 \tag{18}$$

Results and discussion

This simulation test mainly selected the most obvious characteristic dynamic elastic modulus, elastic modulus and shear modulus ratio, acoustic radiation damping coefficient and acoustic impedance as the input variables of the model, and took the selected material corresponding to the high, medium and low levels of the musical instrument assessed by experts as the output variables to conduct grade simulation analysis on the vibration performance of the national musical instrument soundboard material. According to the national standard of People's Republic of China (PRC) "Subjective Evaluation Method and Technical Index of Sound Quality of Radio Programs" (GB/T 16463-1996), the samples of the test set were graded by five grades, that is, "first class" was 5 points, which meant excellent sound quality. "Second class" was 4 points, which meant that the sound quality was very good. "Third class" was 3 points, which meant that the sound quality was good. "Fourth class" was recorded as 2 points, which meant that the sound quality was average. "Fifth class" was scored as 1 point, which meant poor sound quality. According to the professional sound quality evaluation data: beautiful timbre, bright treble, soft mid-range, rich bass, coherent range, pure sound, and performance level, these seven contents were scored on the spot. According to the score from high to low, each instrument was divided into 1 to 9 levels, of which 1 to 3 levels were defined as high-grade instruments, 4 to 6 levels were

defined as mid-range instruments, and 7 to 9 levels were defined as low-grade instruments.
In the experiment, 90 groups of each sample of the four kinds of wood were taken as the training set, and 60 groups of each sample were taken as the test set. BP and ACO-BP algorithms were used to conduct experiments, and the training results are shown in Fig. 6.

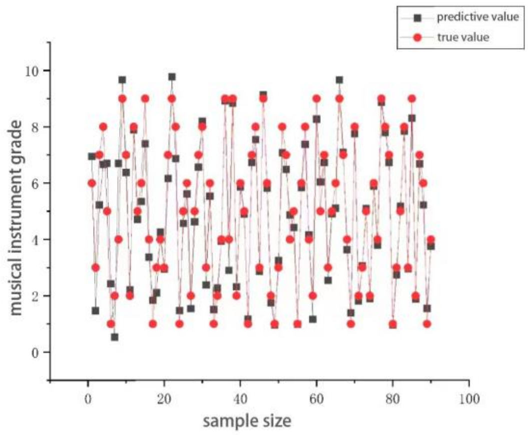

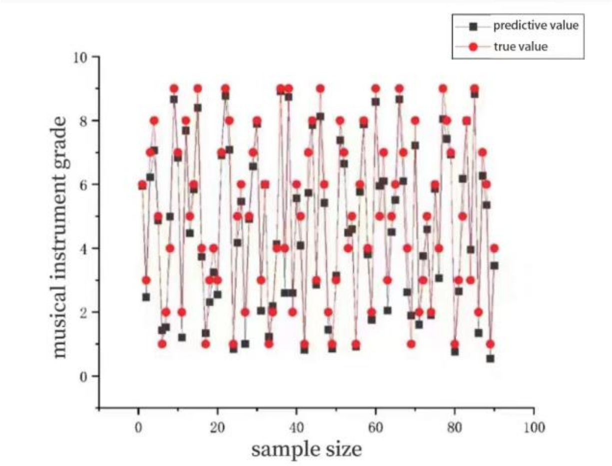

(a) BP neural network prediction result (b) ACO-BP neural network prediction result

Fig. 6 Experimental result

The experimental results in Fig. 6 showed that the BP neural network had a large error in forecasting data and a poor forecasting effect. The BP neural network optimized by ACO had small prediction data error and high prediction accuracy. In Fig. 6 (a), the maximum error between the predicted data of BP neural network and the true value was about 1.5, and the prediction accuracy was 86.7%. In Fig. 6 (b), the prediction accuracy of ACO-BP neural network reached 98%.
The stability of BP algorithm and ACO-BP algorithm in the iteration process was compared, and the training iteration diagram is shown in Fig. 7.

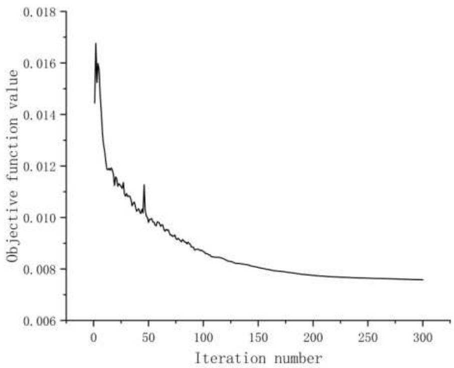

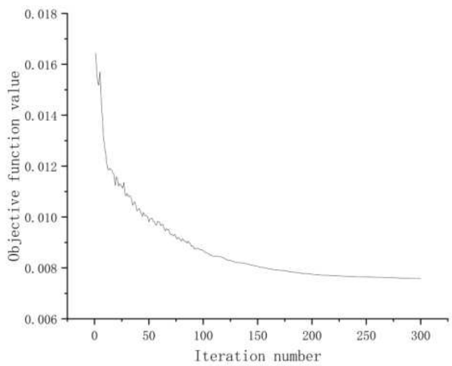

(a) Iterative process of BP neural network training (b) Iterative process of ACO-BP neural network training

Fig. 7 Iterations of algorithm and MSE

Fig. 7(a) shows the training iteration diagram of the BP neural network. Its iteration process fluctuated greatly, its training result was poor, and its prediction result cannot meet the expectation. Fig. 7 (b) illustrates the training iteration diagram of ACO-BP algorithm, showing that the training process was gentle and the training effect was good.

The evaluation grade of the ACO-BP neural network output was divided as follows: the "high" output is [A]; Level "medium" output is [B]; Level "low" output is [C]. The test results of 60 test sets are shown in Table 4.

Table 4 Experimental result of ACO-BP algorithm

	Evaluation level		
	[A]	[B]	[C]
True grade	13	36	11
Forecast grade	13	34	10
accuracy rate		95%	

The result showed that the accuracy of ACO-BP algorithm on the test set was 95%, and the prediction effect was in line with the expectation.

Conclusions

In this study, ACO-BP algorithm was used to evaluate the acoustic quality of piano soundboards by inputting physical parameters of the soundboards. This method eliminated the manual evaluation that was based on people experiences, making the evaluation more intelligent and more scientific and objective, greatly increasing the speed of evaluation. In this study, the ant colony algorithm was used to optimize the BP neural network, which can avoid falling into local minimum and make the prediction result more accurate. This study provided an objective method to evaluate the acoustic quality grade of the music soundboards with high accuracy, which can provide a theoretical basis for the prediction of the soundboard grade of piano.

Declarations

Funding: The work was supported by China Postdoctoral Science Foundation (2019M651240), and National Natural Science Foundation of China (31670559)

Conflicts of interest/Competing interests: I/We have no competing interests.

Availability of data and material: Due to project requirements, the basic data in this article cannot be publicly shared.

Code availability: Declarations

Authors' contributions: Declarations

Ethics approval: Declarations

Consent to participate: Declarations

Consent for publication: Declarations

References

[1]Y Yang, Z Liu, Y J J o F R Liu. Prediction of lute acoustic quality based on soundboard vibration performance using multiple choice model[J], 2017, 28: 855-861.

[2]C Buksnowitz,A Teischinger,U Müller,A Pahler,R J T j o t a s o A Evans. Resonance wood [Picea abies (L.) Karst.]–evaluation and prediction of violin makers' quality-grading[J], 2007, 121(4): 2384-2395.

[3]J J R o P i P Woodhouse. The acoustics of the violin: a review[J], 2014, 77(11): 115901.

[4]P Horcin,V Gubriansky. Properties of wood in musical instruments making[C]. Forum Acusticum, 2005 : .

[5]J Berthaut,M Ichchou,L J A A Jezequel. Piano soundboard: structural behavior, numerical and experimental study in the modal range[J], 2003, 64(11): 1113-1136.

[6]H Suzuki,I J A A Nakamura. Acoustics of pianos[J], 1990, 30(2-3): 147-205.

[7]C M J M b Hutchins. Measurable characteristics of violin-family instruments in relation to the sound of a high-quality violin[J], 1995, 20(3): 29-31.

[8]I J T J o t A S o A Brémaud. Acoustical properties of wood in string instruments soundboards and tuned idiophones: Biological and cultural diversity[J], 2012, 131(1): 807-818.

[9]I J A Bremaud. What do we know on" resonance wood" properties? Selective review and ongoing research[J], 2012, : .
[10]T Ono,M J J j o A p Norimoto. Study on Young's modulus and internal friction of wood in relation to the evaluation of wood for musical instruments[J], 1983, 22(4R): 611.
[11]E Obataya,T Ono,M J J o M S Norimoto. Vibrational properties of wood along the grain[J], 2000, 35(12): 2993-3001.
[12]Y Kubojima,T Okano,M J J o W S Ohta. Bending strength and toughness of heat-treated wood[J], 2000, 46: 8-15.
[13]N J M G SOBUE. INSTANTANEOUS MEASUREMENT OF ELASTIC-CONSTANTS BY ANALYSIS OF THE TAP TONE OF WOOD-APPLICATION TO FLEXURAL VIBRATION OF BEAMS[J], 1986, 32(4): 274-279.
[14]N J M G Sobue. Measurement of Young's modulus by the transient longitudinal vibration of wooden beams using a fast Fourier transformation spectrum analyzer[J], 1986, 32: 744-747.
[15]N J J o t J W R S Sobue. Simultaneous determination of Young's modulus and shear modulus of structural lumber by complex vibrations of bending and twisting[J], 1988, : .
[16]N Sobue,M J 木 Kitazumi. Identification of power spectrum peaks of vibrating completely-free wood plates and moduli of elasticity measurements[J], 1991, 37(1): 9-15.
[17]B W Smith,J Dalen,K Wiggins,E Tooley,P Christopher,J J I j o b m Bernard. The brief resilience scale: assessing the ability to bounce back[J], 2008, 15: 194-200.
[18]M J S u Buscema,misuse. Back propagation neural networks[J], 1998, 33(2): 233-270.
[19]M Dorigo,M Birattari,T J I c i m Stutzle. Ant colony optimization[J], 2006, 1(4): 28-39.